

Recombinant yeast VDAC2: a comparison of electrophysiological features with the native form

Andrea Magri^{1,2}, Andonis Karachitos³, Maria Carmela Di Rosa², Simona Reina², Stefano Conti Nibali¹, Angela Messina^{2,4}, Hanna Kmita³ and Vito De Pinto^{1,4}

1 Department of Biomedical and Biotechnological Sciences, University of Catania, Italy

2 Department of Biological, Geological and Environmental Sciences, Section of Molecular Biology, University of Catania, Italy

3 Department of Bioenergetics, Faculty of Biology, Institute of Molecular Biology and Biotechnology, Adam Mickiewicz University, Poznan, Poland

4 National Institute for Biomembranes and Biosystems, Section of Catania, Italy

Keywords

electrophysiology; heterologous expression; mitochondria; mitochondrial porins; planar lipid bilayer; VDAC2; yeast; yeastVDAC2; yVDAC2

Correspondence

A. Magri, Department of Biological, Geological and Environmental Sciences, Section of Molecular Biology, University of Catania, V. le Andrea Doria, 6, Cittadella Universitaria, 95125, Catania, Italy
E-mail: andrea.magri@unict.it

Andrea Magri and Andonis Karachitos contributed equally to this work

(Received 6 August 2018, revised 4 December 2018, accepted 10 December 2018)

doi:10.1002/2211-5463.12574

Voltage-dependent anion channel isoform 2 of the yeast *Saccharomyces cerevisiae* (yVDAC2) was believed for many years to be devoid of channel activity. Recently, we isolated yVDAC2 and showed that it exhibits channel-forming activity in the planar lipid bilayer system when in its so-called native form. Here, we describe an alternative strategy for yVDAC2 isolation, through heterologous expression in bacteria and refolding *in vitro*. Recombinant yVDAC2, like its native form, is able to form voltage-dependent channels. However, some differences between native and recombinant yVDAC2 emerged in terms of voltage dependence and ion selectivity, suggesting that, in this specific case, the recombinant protein might be depleted of post-translational modification(s) that occur in eukaryotic cells.

The voltage-dependent anion channel (VDAC) proteins, also known as mitochondrial porins, are the most abundant proteins in the mitochondrial outer membrane (MOM) of all eukaryotes. Characterized by a molecular mass of 30–32 kDa, VDAC proteins allow for the continuous exchange of metabolites (ATP/ADP, NAD⁺/NADH, Krebs cycle intermediates) and ions (Na⁺, Cl⁻, Mg²⁺, Ca²⁺) between mitochondria and cytosol. Therefore, they play a crucial role in mitochondrial bioenergetics [1–3]. In mammals, where

three different but conserved isoforms are expressed (VDAC1, VDAC2 and VDAC3) [4], evolution has conferred to each isoform peculiar additional functions beyond the metabolic role. For example, VDAC1 and VDAC2 participate differently in the regulation of cell death [5–8], while recent literature suggests the involvement of VDAC3 in reactive oxygen species (ROS) homeostasis [9,10]. The three-dimensional structure of mammalian VDAC1 has been shown to involve a transmembrane β -barrel structure, formed by 19

Abbreviations

LDAO, lauryldimethylamine oxide; MOM, mitochondrial outer membrane; PLB, planar lipid bilayer; PTM, post-translational modification; ROS, reactive oxygen species; VDAC, voltage-dependent anion channel; yVDAC2, yeast voltage-dependent anion channel isoform 2.

amphipathic, mostly anti-parallel β -strands, with the exception of the N-terminal domain, which is structured as an α -helix and partially exposed to the cytosol [11–13]. A similar result was obtained for zebrafish VDAC2 [14] and for other species by homology modeling studies [15], suggesting a conserved structure of VDAC across evolution.

Differently from mammals, the budding yeast *Saccharomyces cerevisiae* has only two distinct VDAC genes, *POR1* and *POR2*, encoding two different VDAC isoforms. However, only yVDAC1 is widely considered essential for mitochondrial metabolism. Indeed, the inactivation of the *POR1* gene, as in the $\Delta por1$ mutant strain, resulted in a strong inhibition of cell growth in non-fermentable conditions, especially at the restrictive temperature of 37 °C [16]. On the contrary, the inactivation of the *POR2* gene resulted in an undetectable phenotype, since $\Delta por2$ cells were able to grow in a comparable way to the wild-type [16]. Overall, the channel-forming ability of yeast voltage-dependent anion channel isoform 2 (yVDAC2) has been questioned for many years. Contrasting results were indeed obtained upon *POR2* overexpression; namely, a complete recovery of $\Delta por1$ yeast growth on glycerol was detected [16,17], suggesting a channel activity for yVDAC2, at least under particular conditions. Only recently, an electrophysiological analysis has clearly shown that yVDAC2 is able to form channels in artificial membranes, with features resembling many other members of the VDAC family [18].

In a previous work, we purified yVDAC2 directly from mitochondria extracted from $\Delta por1$ cells overexpressing *POR2*, under native conditions [18]. In parallel, the same protein was prepared by heterologous expression in a bacterial system, purified and refolded as previously performed for many other VDAC isoforms and mutants [19–22]. In this work, we analyzed the electrophysiological features of the recombinant yVDAC2. Our results indicate that the protein is able to form channels in artificial membranes, with similar features to native one but, at the same time, with differences in terms of voltage sensitivity and ion selectivity.

Materials and methods

Cloning of yVDAC2

The sequence encoding yVDAC2 was obtained by reverse transcription from the total RNA previously extracted from *S. cerevisiae* BY4742 (EUROSCARF, Frankfurt, Germany). Reverse transcription was performed by using the AffinityScript Multi-Temp RT and RT-PCR system

(Agilent, Santa Clara, CA, USA) according to the manufacturer's protocol. The corresponding cDNA was amplified by PCR using the following primers: forward 5'-TTTTGCTAGCATGGCACTACGATTTTTCAACGAT-3' and reverse 5'-TTTTCTCGAGGGGCGAGAACGATAGAGACCA-3'. The yVDAC2 cDNA was cloned in the bacterial expression vector pET-21b (Novagen, Madison, WI, USA) by *NheI/XhoI* digestion, in frame with the His-tag at the C-terminal part. The construct was verified by sequencing.

Expression, purification and refolding of yVDAC2 protein

Escherichia coli BL21 (DE3) cells were transformed with pET-21b plasmid containing the yVDAC2 sequence. Transformed cells were grown to an optical density ($\lambda = 600$ nm) of 0.6, and the protein expression was induced by addition of 0.4 mM isopropyl- β -D-thiogalactopyranoside (IPTG) (Sigma-Aldrich, Saint Louis, MO, USA), for 3 h at 30 °C. Cells were harvested by centrifugation and lysed in buffer B (8 M urea, 1 mM NaH_2PO_4 , 0.01 mM Tris/HCl, pH 8.0) overnight at 4 °C. The total protein lysate was clarified by centrifugation and loaded onto Ni-NTA agarose (Thermo Fisher Scientific, Waltham, MA, USA) packed column, previously equilibrated with buffer B. The column was then washed twice with five volumes of buffer C (8 M urea, phosphate buffer, pH 6.3), and proteins were purified by elution with five volumes of buffer E (8 M urea, phosphate buffer, pH 3.5). The eluted protein was refolded by incubation at 4 °C in a 10-fold volume of refolding buffer [25 mM Tris, 100 mM NaCl, 1 mM EDTA, 1% (v/v) lauryldimethylamine oxide (LDAO, Sigma-Aldrich), pH 7.0]. Then, the protein solution was dialyzed against 100 volumes of a dialysis buffer (25 mM Tris, 1 mM EDTA, 0.1% LDAO, pH 7.0) with Thermo Scientific Slide-A-Lyzer Dialysis Cassettes (Thermo Fisher Scientific) (3.5 K MWCO). The solution containing the refolded proteins was clarified by centrifugation (60 000 g, 1 h) and loaded into a size exclusion chromatography column (Superdex 200 Increase 30/100, GE Healthcare, Chicago, IL, USA) in SEC buffer (150 mM NaCl, 20 mM Tris/HCl, pH 8.0, 1 mM DTT 0.1% LDAO) to separate aggregates from monomers. Elution fractions, corresponding exclusively to the monomer peak, were collected.

Electrophysiological analysis of recombinant yVDAC2

The refolded yVDAC2 was reconstituted into a planar lipid bilayer (PLB) system as previously described in [20–22]. Bilayers of approximately 80–100 pF capacity made of asolectin from a soybean phospholipid mixture (Sigma-Aldrich) at a concentration of 20 mg·mL⁻¹ in *n*-decane were used. Channel insertion was obtained by addition of

0.5–5 μ L of protein solution to the *cis* side of the cuvette containing approximately 3 mL of aqueous solution (1 M KCl, 10 mM Hepes, pH 7.0). Data were acquired using a Bilayer Clamp amplifier (Warner Instruments, Hamden, CT, USA) at 100 μ s per point, filtered at 300 Hz and analyzed offline using the PCLAMP program set (version 10; Molecular Devices, San Jose, CA, USA). Channel conductance (G) was calculated from current (I) measurements in the presence of an applied constant voltage (V_m) of +10 mV, as the I/V_m ratio. Distribution of conductance was obtained from six independent reconstitution experiments, each showing several channel insertions.

Voltage dependence analysis of γ VDAC proteins

Analysis of voltage dependence of recombinant γ VDAC2 was performed in 1 M KCl, 10 mM Hepes, pH 7.0, by application of two distinct voltage ramps including positive and negative potentials (amplitude ± 90 mV, time 100 s). At least three independent multi-channel experiments were performed. Values of G and G_{max} , indicating respectively the conductance value at a given V_m and the maximal conductance, were calculated for the recombinant γ VDAC2. Control experiments were performed using the native γ VDAC1 and γ VDAC2 produced as previously described [18]. The relative conductance was calculated as the G/G_{max} ratio and plotted as a function of the voltage using PRISM 7 software (GraphPad Software Inc., La Jolla, CA, USA). Three independent experiments were performed for each protein and data are shown as the mean \pm SEM.

Ion selectivity measurement of γ VDAC2

Selectivity measurements were performed for the recombinant γ VDAC2 in a 0.1 M/1 M *cis/trans* gradient of KCl in a voltage range of ± 90 mV, by increasing V_m with discrete steps of ± 5 mV for 45 s. Values of conductance were plotted as a function of V_m , and linear regression was applied with PRISM 7 software. The permeability ratio of cation K^+ (P_C) over anion Cl^- (P_A) was calculated from the reversal potential (V_r) using the Goldman–Hodgkin–Katz equation, according to [23]. Six independent selectivity measurements were performed with both a single- and a multi-channel approach.

Results

Reconstituted recombinant γ VDAC2 forms channels of conductance similar to the native protein

To analyze the electrophysiological properties of recombinant γ VDAC2, the corresponding encoding sequence was introduced into *E. coli* BL21 (DE3) cells

and the protein expression was achieved by IPTG induction, as verified by SDS/PAGE (Fig. 1A). The recombinant protein was extracted directly from inclusion bodies and purified by nickel affinity chromatography, exploiting the 6 \times His tag (Fig. 1B). Since the heterologous expression of membrane proteins in bacterial systems leads to loss of proper conformation and activity, the purified γ VDAC2 was refolded and dialyzed. In order to avoid the presence of aggregates in the final protein solution, size exclusion chromatography was performed and the elution fractions, corresponding to the monomers (Fig. 1C), were collected and used in our study. Finally, the electrophysiological features of recombinant γ VDAC2 were analyzed at the PLB.

The representative current trace displayed in Fig. 2A clearly shows that recombinant γ VDAC2 was able to form channels in artificial membrane, since insertion of three different channels of similar size in a short time was obtained after the addition of the protein solution to the *cis* side of the cuvette. The histogram in Fig. 2B shows the distribution of conductance values calculated for $n = 36$ channels. The analysis, performed in 1 M KCl, 10 mM Hepes, pH 7, in the presence of an applied constant voltage of +10 mV, allowed for calculation of the average conductance, estimated as 3.76 ± 0.94 nS (SD, $n = 36$). This value perfectly overlaps our previous measurements showing an average conductance for the native γ VDAC2 of about 3.6 nS in the same experimental conditions [18]. Overall, our results indicate that, in artificial membrane, recombinant γ VDAC2 forms channels of conductance similar to the native protein.

Recombinant γ VDAC2 is less sensitive to the applied voltage than the native protein

It is known that the conductance of VDAC proteins changes depending on the applied voltage. This feature, well conserved through evolution from yeast to human, is known as voltage dependence. In general, yeast or mammalian VDAC1 persists at low potentials in a stable highly conductive state, called the ‘open’ state. However, as the applied voltage rises (starting from ± 20 – 30 mV), VDAC1 switches to several low-conducting states, called ‘closed’ states [24–27]. We demonstrated previously that the native γ VDAC2 shows a less pronounced voltage dependence in comparison to γ VDAC1, because γ VDAC2-formed channel closure began from ± 40 – 50 mV of applied voltage [18].

In order to analyze the effect of voltage on recombinant γ VDAC2 conductance, PLB experiments were

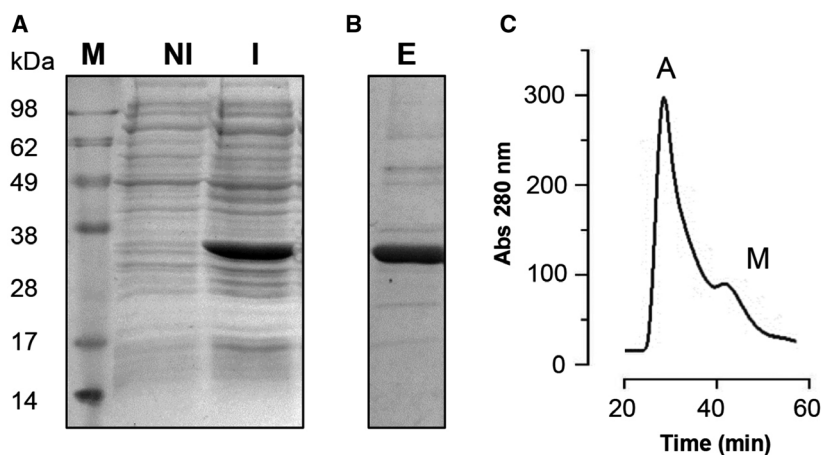


Fig. 1. Expression and purification of γ VDAC2 in bacterial system. (A) SDS/PAGE analysis of whole *Escherichia coli* BL21 (DE3) lysate from cells transformed with the pET-21b- γ VDAC2 construct, obtained in the presence of 0.4 M IPTG (I, induced). As a control, a sample that was not induced (NI) was used. Addition of IPTG allowed the expression of recombinant γ VDAC2 as demonstrated by the strong band of the expected molecular mass (28–32 kDa) exclusively found in the induced sample. 'M' indicates the molecular mass marker. (B) SDS/PAGE of eluate (E) obtained after Ni-NTA chromatography of the total induced lysate. As shown, a predominant band of the expected molecular mass was detected. (C) Elution profile obtained by size-exclusion chromatography of refolded protein. 'A' indicates the peak corresponding to aggregated proteins; 'M' indicates the peak corresponding to the monomeric protein. Only fractions corresponding to monomeric protein were collected and used going forward.

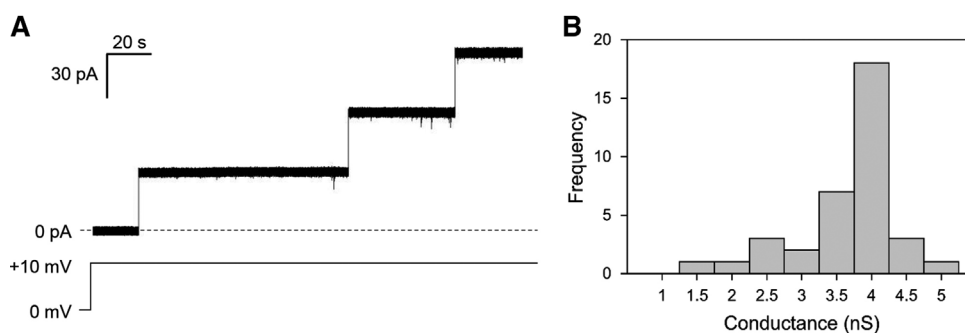


Fig. 2. Pore-forming activity analysis of recombinant γ VDAC2 in artificial membranes. (A) Representative trace of γ VDAC2 activity recorded at the PLB. Channels insertion was achieved after addition of 0.5–5 μ L of protein solution into the *cis* side of the cuvette, in presence of a lipid bilayer. Discrete steps indicate single channel insertion. Experiment was performed in 1 M KCl, 10 mM Hepes, pH 7, at a constant applied voltage of +10 mV. (B) Distribution of conductance values obtained for $n = 36$ channels inserted in the membrane. Most of the channels showed conductance values between 3.5 and 4 nS, resulting in an average conductance value of 3.76 ± 0.94 nS (SD, $n = 36$).

performed by the application of voltage ramps from 0 to ± 90 mV. The curves, displayed in Fig. 3A, indicate that recombinant γ VDAC2 is completely insensitive to low positive and negative voltages, since no closure was detected either at potentials that normally close yeast or mammalian VDAC1 or at voltages able to close native γ VDAC2. Only the application of high voltages, starting from ± 70 – 80 mV, induced a channel closure, which occurred symmetrically at both positive and negative potentials, suggesting that recombinant γ VDAC2 is significantly less voltage sensitive than the native protein. Furthermore, current across recombinant γ VDAC2 was monitored upon application of the

constant voltage +90 mV. As shown in the representative trace in Fig. 3B, a complete closure of the channels occurred only after a prolonged exposure to high potential, highlighting the recombinant γ VDAC2 limited sensitivity to voltage.

The electrophysiological behavior of the native protein was then analyzed in the presence of similar high voltages, by applying a voltage ramp from 0 to +90 mV. According to our previous data [18], native γ VDAC2 began to close around +40–50 mV, as shown by the trace in Fig. 4A. However, the application of higher potentials (i.e. +80 mV) promoted a further channel closure, similarly to that previously shown by the recombinant

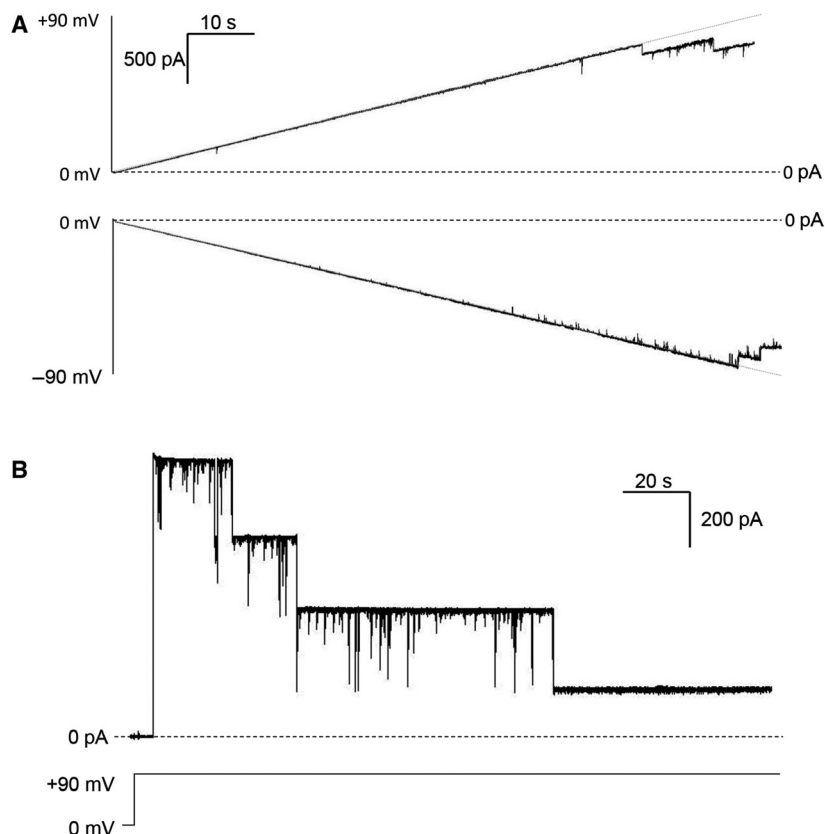


Fig. 3. Voltage dependence of recombinant γ VDAC2. (A) Representative traces of γ VDAC2 activity at the PLB in presence of voltage ramps from 0 to +90 mV (upper trace) and from 0 to -90 mV (lower trace). Traces show that no change in the conductance was obtained at low positive or negative potentials. A significant reduction of channel conductance was obtained starting from ± 80 mV. Experiments were performed in 1 M KCl, 10 mM Hepes, pH 7. (B) Representative trace of recombinant γ VDAC2 recorded at the constant voltage of +90 mV for a prolonged time; $n = 3$ different channels inserted in the membrane. It is clear that application of high voltage promotes a step-by-step closure of γ VDAC2 channels. The experiment was performed in 1 M KCl, 10 mM Hepes, pH 7.

protein (see Fig. 3A). To deeply analyze this aspect, the values of conductance (G) obtained at each applied voltage for both native and recombinant proteins, as well as for the native γ VDAC1, were normalized relative to the maximal conductance (G_{\max}). Then, as shown in Fig. 4B, relative conductance values (G/G_{\max}) were plotted as a function of the applied voltage (amplitude of ± 90 mV). As expected, γ VDAC1 conductance (pale green circles) significantly decreased starting from ± 20 – 30 mV, reaching a stable level of closure characterized by a decrease at about 50% of the maximal conductance. Native γ VDAC2 (orange circles) began to close around ± 40 – 50 mV and its conductance at these voltages showed a decrease of about 20%, in a similar manner to that shown previously [18]. It is clear that this channel is not able to reach a channel closure similar to that observed for γ VDAC1. However, the application of high voltages, up to ± 80 – 90 mV, promoted a further 10–15% decrease of its relative conductance.

The results shown in Fig. 4B also confirmed the overall attenuation of voltage dependence in the case of recombinant γ VDAC2 (red circles) observed in Fig. 3. Furthermore, the application of voltages up to ± 60 – 70 mV did not promote any significant decrease in the channel conductance. Conversely, the application of potentials ± 80 – 90 mV caused channel closure, as G/G_{\max} values almost overlap those calculated for both native γ VDAC1 and γ VDAC2 at similar voltages. Although the recombinant γ VDAC2 still shows voltage dependence, our results suggest a decrease of voltage sensitivity even with respect to the native form.

Recombinant γ VDAC2 displays exclusively cation-selective states

It is known that VDAC displays an anionic selectivity in the high-conducting ‘open’ state and a less anionic or more cationic selectivity in the low-conducting

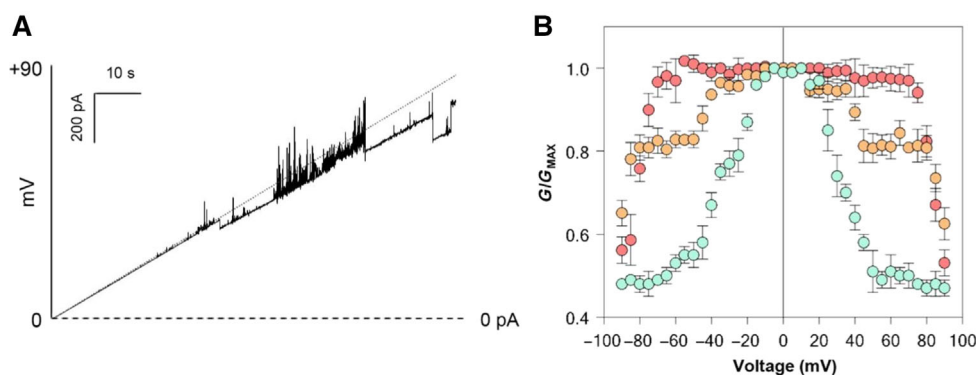


Fig. 4. Comparative analysis of relative conductance for γ VDAC proteins. (A) A representative trace of native γ VDAC2 activity in presence of voltage ramps from 0 to +90 mV. The trace shows that the protein undergoes to partial closure at +40–50 mV and, as the voltage increases, channels become noisy. However, a stable reduction of channel conductance was obtained starting from ± 80 mV. Experiments were performed in 1 M KCl, 10 mM Hepes, pH 7. (B) Analysis of relative conductance (G/G_{\max}) (\pm SEM) of $n = 3$ independent experiments showing the different voltage-dependent features of γ VDAC proteins. Pale green circles refer to γ VDAC1, orange circles refer to native γ VDAC2 results, and red circles refer to recombinant γ VDAC2. As reported, both native and recombinant γ VDAC2 remain in an open state up to application of high voltages, starting from ± 80 –90 mV, when they switch to the closed state. Experiments were performed in 1 M KCl, 10 mM Hepes, pH 7.

‘closed’ state [28,29]. In the previous work, the presence of 1 and 0.1 M KCl in the *cis* and *trans* side of the cuvette, respectively, allowed for detection of the presence of different selectivity states, three in total for native γ VDAC2. Two of them appeared to be high-conducting states but with an opposite selectivity, while the third was a very low-conducting state characterized by an extremely pronounced cation selectivity [18]. In order to analyze the ion selectivity of recombinant γ VDAC2, current values, measured in a 10-fold gradient of KCl and obtained upon application of discrete voltages in the range of ± 90 mV, were plotted as a function of the applied voltage. Linear regressions of the obtained data (Fig. 5) indicated the presence of only two distinct states of recombinant γ VDAC2, i.e. a main high-conducting state (called state 1 in Fig. 5) and a low-conducting state (state 2 in Fig. 5) and that both states displayed a cation selectivity.

The Goldman–Hodgkin–Katz equation was then used to calculate the ratio between permeability of cations over anions (P_C/P_A) for the two states of recombinant γ VDAC2, using a reversal potential corresponding to the voltage at zero current [23]. The P_C/P_A value obtained for state 1 was 1.94 ± 0.19 and the value obtained for state 2 was 11.2 ± 2.8 . For comparison, the corresponding P_C/P_A values obtained for native γ VDAC2 were 2.17 ± 0.11 and 16.24 ± 6 , respectively [18]. This clearly indicates that recombinant and native γ VDAC2 are very similar in terms of cationic strength. In particular, the lowest conducting state determined for both variants of γ VDAC2 is

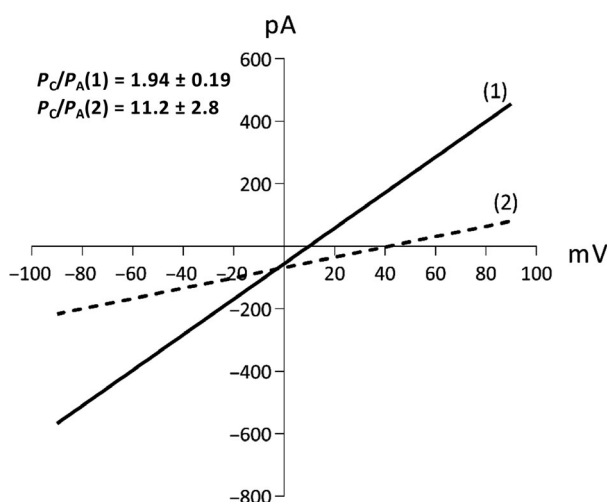


Fig. 5. Ion selectivity of recombinant γ VDAC2. Representative graph of current–voltage relationship of γ VDAC2 recombinant protein performed in 10-fold gradient of 1 M KCl obtained by application of voltage steps for a prolonged time. The conductance (slope) and the reversal potentials were calculated from the extrapolated regression lines of the different conducting states of the channel. The multi-channel experiment shown was performed with $n = 8$ channels inserted in the membrane. Numbers indicate the different states: 1, cationic high-conducting state; 2, cationic low-conducting state.

characterized by a pronounced selectivity for cations over anions, a feature found exclusively for γ VDAC2. At the same time, a significant difference between native and recombinant protein emerged, since no anionic state was found for the recombinant one.

Discussion

So far, the second VDAC isoform of the yeast *S. cerevisiae* has been considered to be one of the most elusive members of the VDAC family. Indeed, since the *POR2* gene discovery, the story of yVDAC2 has been controversial. Differently from *POR1*, the genetic inactivation of *POR2* has no consequence for yeast growth on non-fermentable carbon sources [16]. Furthermore, no data about yVDAC2 reconstitution in liposomes and/or artificial membranes were available for a long time, raising the suspicion (now proved wrong [18]) that the yVDAC2 protein was completely devoid of channel function. On the contrary, the overexpression of the *POR2* gene in $\Delta por1$ cells promoted the restoration of the yeast wild-type growth phenotype. This effect can be achieved when the *POR2* sequence is transcribed under the control of a strong promoter [16] or is activated by an external factor, such as the serendipitously found human SOD1, which stimulates *POR2* overexpression [17]. These findings in turn suggest that the contribution of yVDAC2 to the permeability of the yeast MOM is a consequence of its expression level, providing a logical explanation for the recovery of $\Delta por1$ cell growth [16] and of the mitochondrial functionality [17]. To definitively clarify the functional properties of yVDAC2, we have recently analyzed the electrophysiological features of this protein reconstituted into artificial membranes by using two parallel approaches. As shown in our previous work, we isolated yVDAC2 directly from $\Delta por1$ mitochondria, after yeast cell transformation with an expression plasmid carrying the corresponding yVDAC2 cDNA sequence. This strategy allowed us to increase *POR2* transcript concentration and consequently the corresponding protein amount, which simplified the protein isolation under the native condition [18]. Alternatively, yVDAC2 was produced as a recombinant protein in *E. coli* cells, a procedure commonly used for large-scale protein production, since it allows a high yield of protein to be obtained in a relatively short time with minimal cost and effort. The same approach was previously used by our group for the characterization of human VDAC3 [20] and its cysteine mutants [21], and for the production of human VDAC1 suitable for interaction studies with proteins involved in neurodegenerative diseases [22,30]. Furthermore, an identical approach was used by Hiller and coauthors to obtain the human VDAC1 preparation for NMR studies aimed at identifying its three-dimensional structure [11,31] and by Abramson's group to purify the mouse VDAC1, later crystalized [13], confirming the strength of this method. With this

perspective, the yVDAC2 cDNA was cloned into a specific expression vector and the protein was expressed in bacterial cells. Since membrane proteins localize into inclusion bodies, bacterial lysis occurred upon denaturing conditions, with the loss of the native conformation. Therefore, once isolated, in order to obtain a perfectly active protein, the recombinant protein must undergo a refolding procedure using a well-established protocol [11,19–22].

Recombinant yVDAC2 was then characterized by reconstitution in a PLB system and previous data were used as a reference. Our reconstitution experiments clearly indicate the ability of the recombinant protein to form channels in artificial membranes, with an average conductance value identical to that previously found for the native protein. This result confirmed also the appropriateness of our refolding method. The analyses of voltage dependence indicate that the recombinant yVDAC2 is less sensitive to voltage than native yVDAC1 and yVDAC2, although the voltage dependence of the latter is also weaker than that of the former. Accordingly, only application of a high potential is able to promote a strong attenuation (approximately halving) of relative conductance of native yVDAC2, allowing the protein to reach a similar closure level to that displayed by yVDAC1. Similarly, the recombinant yVDAC2 undergoes a complete and stable closure exclusively at high potentials, such as ± 80 – 90 mV.

Another significant difference among native and recombinant yVDAC2 concerns ion selectivity. In our previous work, we found that native yVDAC2 displays the anion-selective state typical of most VDAC proteins, and two different cation-selective states [18]. Importantly, both cation-selective states are observed for recombinant yVDAC2 as indicated by values of P_C/P_A , but no anion-selective state was found for the recombinant protein. Although the presence of the highly conductive cationic state was already observed in VDAC1 extracted from *Neurospora crassa* or rat liver mitochondria [32], such a difference between native and recombinant VDAC1 from yeast or human has not been detected so far; rather many papers agree with the fact that both samples behave similarly upon PLB analysis in terms of conductance, voltage dependence and selectivity. Conversely, specific functional differences were noticed in the case of human VDAC3. The first electrophysiological characterization of VDAC3 was obtained by heterologous expression in bacteria, which produced proteins able to form pores in artificial membranes with a very low conductance (100 pS in 1 M KCl, channels about 35–40 times smaller than both VDAC1 and VDAC2) [20]. However, the work by Okazaki *et al.* showed that the

recombinant VDAC3 could form channels with conductance similar to the other isoforms [33]. In this work, although the proteins were obtained with very similar protocols, the presence of reducing agents in preparation buffers and in PLB experiments led to the formation of channels of normal conductance. Moreover, channels of regular conductance were also obtained by using human VDAC3 directly extracted in the same conditions from yeast mitochondria [27]. At variance was that VDAC3 purified in the absence of reducing agents showed different electrophysiological features [21]. The reason for such differences was later attributed to the presence of specific post-translational modifications (PTMs), in particular to irreversible oxidation states of cysteine residues, as demonstrated by electrophysiological characterization in [21] and recently confirmed by high-resolution mass spectrometry [34,35].

We thus hypothesize that also the differences between native and recombinant γ VDAC2 could be explained by naturally occurring PTMs. While the native protein is isolated directly from yeast mitochondria under native conditions, the recombinant protein is produced in a heterologous system lacking any eukaryotic PTMs. Beyond oxidation, VDAC proteins undergo phosphorylation of specific amino acid in both physiological and pathological conditions [36,37], which could be responsible for modulation of voltage sensitivity, as well as other electrophysiological parameters, as has been recently proposed [38,39]. Furthermore, it is known that modifications of amino acid residues change VDAC features. For instance, the treatment of VDAC1 with succinic anhydride abolishes the voltage dependence and changes its selectivity from an anionic to a cationic one [40].

In conclusion, the slight functional differences found in the specific case of *S. cerevisiae* VDAC2 between the native and recombinant proteins do not affect the biological significance of our findings, indicating that γ VDAC2 is definitely another member of the VDAC family, being able to form voltage-dependent channel of about 3.6 nS conductance under our experimental conditions. The behavior of the recombinant protein supports our hypothesis of the presence of specific PTMs in the native one. As a further, intriguing consequence, our results indicate that such differences could be associated to the still unknown role of γ VDAC2. Its encoding gene is under-expressed in normal conditions. It is not the first time, indeed, that an under-expressed isoform of VDAC was noticed, as was recently found in *Drosophila melanogaster*: in that case, a regulatory function has been associated to the alternative isoform [41].

Acknowledgements

The authors acknowledge the financial support of MIUR PRIN, project 2015795S5W_005, Piano della Ricerca UNICT 2017 to VDP and A. Messina, Fondazione Umberto Veronesi for a post-doctoral fellowship to A Magrì.

Conflict of interest

The authors declare no conflict of interest.

Author contributions

A. Magrì, AK, and SR performed electrophysiological experiments. A. Magrì, MCDR, and SCN performed protein purification. A. Magrì, A. Messina, HK, and VDP analyzed the data and wrote the manuscript.

References

- 1 Benz R (1994) Permeation of hydrophilic solutes through mitochondrial outer membranes: review on mitochondrial porins. *Biochim Biophys Acta* **1197**, 167–196.
- 2 Colombini M (2004) VDAC: the channel at the interface between mitochondria and the cytosol. *Mol Cell Biochem* **256–257**, 107–115.
- 3 Shoshan-Barmatz V, De Pinto V, Zweckstetter M, Raviv Z, Keinan N and Arbel N (2010) VDAC, a multi-functional mitochondrial protein regulating cell life and death. *Mol Asp Med* **31**, 227–285.
- 4 Messina A, Reina S, Guarino F and De Pinto V (2012) VDAC isoforms in mammals. *Biochim Biophys Acta* **1818**, 1466–1476.
- 5 Granville DJ & Gottlieb RA (2003) The mitochondrial voltage-dependent anion channel (VDAC) as a therapeutic target for initiating cell death. *Curr Med Chem* **16**, 1527–1533.
- 6 Shoshan-Barmatz V, Zakar M, Rosenthal K & Abu-Hamad S (2009) Key regions of VDAC1 functioning in apoptosis induction and regulation by hexokinase. *Biochim Biophys Acta* **1787**, 421–430.
- 7 Magrì A, Reina S and De Pinto V (2018) VDAC1 as pharmacological target in cancer and neurodegeneration: focus on its role in apoptosis. *Front Chem* **6**, 108.
- 8 Cheng EH, Sheiko TV, Fisher JK, Craigen WJ and Korsmeyer SJ (2003) VDAC2 inhibits BAK activation and mitochondrial apoptosis. *Science* **301**, 513–517.
- 9 De Pinto V, Reina S, Gupta A, Messina A and Mahalakshmi R (2016) Role of cysteines in mammalian VDAC isoforms' function. *Biochim Biophys Acta* **1857**, 1219–1227.

- 10 Reina S, Guarino F, Magrì A and De Pinto V (2016) VDAC3 as a potential marker of mitochondrial status is involved in cancer and pathology. *Front Oncol* **6**, 264.
- 11 Hiller S, Graces RG, Malia TJ, Orekhov VY, Colombini M and Wagner G (2008) Solution structure of the integral human membrane protein VDAC-1 in detergent micelles. *Science* **321**, 1206–1210.
- 12 Bayrhuber M, Menis T, Habeck M, Becker S, Giller K, Villinger S, Vonrhein C, Griesinger C, Zweckstetter M and Zeth K (2008) Structure of the human voltage-dependent anion channel. *Proc Natl Acad Sci USA* **105**, 15370–15375.
- 13 Ujwal R, Cascio D, Colletier JP, Fahama S, Zhanga J, Torod L, Pinga P and Abramson J (2008) The crystal structure of mouse VDAC1 at 2.3 Å resolution reveals mechanistic insights into metabolite gating. *Proc Natl Acad Sci USA* **105**, 17742–17747.
- 14 Schredelseker J, Paz A, López CJ, Altenbach C, Leung CS, Drexler MK, Chen JN, Hubbell WL and Abramson J (2014) High resolution structure and double electron-electron resonance of the zebrafish voltage-dependent anion channel 2 reveal an oligomeric population. *J Biol Chem* **289**, 12566–12577.
- 15 De Pinto V, Guarino F, Guarnera A, Messina A, Reina S, Tomasello MF, Palermo V and Mazzoni C (2010) Characterization of human VDAC isoforms: a peculiar function for VDAC3? *Biochim Biophys Acta* **1797**, 1268–1275.
- 16 Blachly-Dyson E, Song J, Wolfgang WJ, Colombini M and Forte M (1997) Multicopy suppressors of phenotypes resulting from the absence of yeast VDAC encode a VDAC-like protein. *Mol Cell Biol* **17**, 5727–5738.
- 17 Magrì A, Di Rosa MC, Tomasello MF, Guarino F, Reina S, Messina A and De Pinto V (2016) Overexpression of human SOD1 in VDAC1-less yeast restores mitochondrial functionality modulating beta-barrel outer membrane protein genes. *Biochim Biophys Acta* **1857**, 789–798.
- 18 Guardiani C, Magrì A, Karachitos A, Di Rosa MC, Reina S, Bodrenko I, Messina A, Kmita H, Ceccarelli M and De Pinto V (2018) γ VDAC2, the second mitochondrial porin isoform of *Saccharomyces cerevisiae*. *Biochim Biophys Acta* **1859**, 270–279.
- 19 Reina S, Magrì A, Lolicato M, Guarino F, Impellizzari A, Maier E, Benz R, Ceccarelli M, De Pinto V and Messina A (2013) Deletion of β -strands 9 and 10 converts VDAC1 voltage-dependence in an asymmetrical process. *Biochim Biophys Acta* **1827**, 793–805.
- 20 Checchetto V, Reina S, Magrì A, Szabò I and De Pinto V (2014) Recombinant human voltage dependent anion selective channel isoform 3 (hVDAC3) forms pores with a very small conductance. *Cell Physiol Biochem* **34**, 842–853.
- 21 Reina S, Checchetto V, Saletti R, Gupta A, Chaturvedi D, Guardiani C, Guarino F, Scorciapino MA, Magrì A, Foti S *et al.* (2016) VDAC3 as a sensor of oxidative state of the intermembrane space of mitochondria: the putative role of cysteine residue modifications. *Oncotarget* **7**, 2249–2268.
- 22 Magrì A, Belfiore R, Reina S, Tomasello MF, Di Rosa MC, Guarino F, Leggio L, De Pinto V and Messina A (2016) Hexokinase I N-terminal based peptide prevents the VDAC1-SOD1 G93A interaction and re-establishes ALS cell viability. *Sci Rep* **6**, 34802.
- 23 Krammer EM, Saidani H, Prévost M and Homblè F (2014) Origin of ion selectivity in *Phaseolus coccineus* mitochondrial VDAC. *Mitochondrion* **19**, 206–213.
- 24 Colombini M (1980) Structure and mode of action of a voltage dependent anion-selective channel (VDAC) located in the outer mitochondrial membrane. *Ann N Y Acad Sci* **341**, 552–563.
- 25 Benz R, Schmid A and Dihanich M (1989) Pores from mitochondrial outer membranes of yeast and a porin-deficient yeast mutant: a comparison. *J Bioenerg Biomembr* **21**, 439–450.
- 26 De Pinto V, Benz R, Caggese C and Palmieri F (1989) Characterization of the mitochondrial porin from *Drosophila melanogaster*. *Biochim Biophys Acta* **987**, 1–7.
- 27 Karachitos A, Grobys D, Antoniewicz M, Jedut S, Jordan J and Kmita H (2016) Human VDAC isoforms differ in their capability to interact with minocycline and to contribute to its cytoprotective activity. *Mitochondrion* **28**, 38–48.
- 28 Schein SJ, Colombini M and Finkelstein A (1976) Reconstitution in planar lipid bilayers of a voltage-dependent anion-selective channel obtained from paramecium mitochondria. *J Membr Biol* **30** (2), 99–120.
- 29 Colombini M (2016) The VDAC channel: molecular basis for selectivity. *Biochim Biophys Acta* **1863** (10), 2498–2502.
- 30 Magrì A and Messina A (2017) Interactions of VDAC with proteins involved in neurodegenerative aggregation: an opportunity for advancement on therapeutic molecules. *Curr Med Chem* **24** (40), 4470–4487.
- 31 Hiller S and Wagner G (2009) The role of solution NMR in the structure determinations of VDAC-1 and other membrane proteins. *Curr Opin Struct Biol* **19** (4), 396–401.
- 32 Pavlov E, Grigoriev SM, Dejean LM, Zweihorn CL, Mannella CA and Kinnally KW (2005) The mitochondrial channel VDAC has a cation-selective open state. *Biochim Biophys Acta* **1710**, 96–102.

- 33 Okazaki M, Kurabayashi K, Asanuma M, Saito Y, Dodo K and Sodeoka M (2015) VDAC3 gating is activated by suppression of disulfide-bond formation between the N-terminal region and the bottom of the pore. *Biochim Biophys Acta* **1848**, 3188–3196.
- 34 Saletti R, Reina S, Pittalà MG, Belfiore R, Cunsolo V, Messina A, De Pinto V and Foti S (2017) High resolution mass spectrometry characterization of the oxidation pattern of methionine and cysteine residues in rat liver mitochondria voltage-dependent anion selective channel 3 (VDAC3). *Biochim Biophys Acta* **1859**, 301–311.
- 35 Saletti R, Reina S, Pittalà MGG, Magrì A, Cunsolo V, Foti Sand De Pinto V (2018) Post-translational modification of VDAC1 and VDAC2 cysteines from rat liver mitochondrial. *Biochim Biophys Acta* **1859**, 806–816.
- 36 Kerner J, Lee K, Tandler B and Hoppel CL (2012) VDAC proteomics: post-translation modifications. *Biochim Biophys Acta* **1818**, 1520–1525.
- 37 Lee H, Lara P, Ostuni A, Presto J, Johansson J, Nilsson I and Kim H (2014) Live-cell topology assessment of URG7, MRP6₁₀₂ and SP-C using glycosylatable green fluorescent protein in mammalian cells. *Biochem Biophys Res Commun* **450** (4), 1587–1592.
- 38 Gupta R and Ghosh S (2017) Phosphorylation of purified mitochondrial Voltage-Dependent Anion Channel by c-Jun N-terminal Kinase-3 modifies channel voltage-dependence. *Biochim Open* **4**, 78–87.
- 39 Miglionico R, Gerbino A, Ostuni A, Armentano MF, Monné M, Carosino M and Bisaccia F (2016) New insights into the roles of the N-terminal region of the ABCC6 transporter. *J Bioenerg Biomembr* **48** (3), 259–267.
- 40 Doring D and Colombini M (1985) Voltage dependence and ion selectivity of the mitochondrial channel, VDAC, are modified by succinic anhydride. *J Membr Biol* **83** (1–2), 81–86.
- 41 Leggio L, Guarino F, Magrì A, Accardi-Gheit R, Reina S, Specchia V, Damiano F, Tomasello MF, Tommasino M and Messina A (2018) Mechanism of translation control of the alternative *Drosophila melanogaster* Voltage Dependent Anion Channel 1 mRNAs. *Sci Rep* **8**, 5347.